Adsorption
https://doi.org/10.1007/s10450-019-00075-9

Phenyl siloxane hybrid xerogels: structure and porous texture

P. Moriones[1,2] · J. C. Echeverria[1,2] · B. Parra Jose[3] · J. J. Garrido[1,2]

Received: 17 December 2018 / Revised: 25 March 2019 / Accepted: 26 March 2019

Abstract

The aim of this research is to investigate the effect of phenyltriethoxysilane (PhTEOS) and tetraethoxysilane (TEOS) molar ratios as silicon precursors on the structure and porous texture of xerogels. We have prepared phenyl-silane hybrid xerogels from mixtures of PhTEOS and TEOS at pH 10 and 333 K, using ethanol as a solvent. Characterization techniques include ^{29}Si NMR, FTIR, XRD, FE-SEM, HRTEM, TGA-DSC, helium density, and gas adsorption (N_2 at 77 K and CO_2 at 273 K). In order to assess the contribution of the quadrupolar moment of N_2 and CO_2 in the adsorption we obtained the adsorption–desorption isotherm of Ar at 87.3 K for the xerogel synthesized from 50% PhTEOS. The morphology of xerogels changed from aggregates of spherical particles for 20% PhTEOS to lamellae for samples obtained with PhTEOS percentages equal or larger that 60%. The incorporation of phenyl groups into the xerogel matrix caused an increase in the spacing bond between silicon atoms and led to an intramolecular reaction and the formation of lamellar domains. Increasing the PhTEOS molar ratio in the mixture of silicon precursors produced hybrid xerogels with lower specific surface area, pore volume and characteristic energy. The similarity between the isotherms of N_2 at 77 K and Ar at 87.3 K indicates that the main retention mechanism is physisorption and that the variation in the surface chemistry with the incorporation of phenyl groups doesn't inhibit the retention of N_2.

Keywords Sol–gel · Phenyltriethoxysilane · Hybrid xerogels · Porous texture

1 Introduction

Phenyl-functionalized silica xerogels are used in several fields due to the outstanding properties resulting from integrating in a single material the properties of silica with the phenyl group functionality. For example, silica matrices modified with phenyl groups have been used to entrap active molecules in their pores that confer specific spectral and dynamic properties of the dyes (Levy et al. 2006; Pardo et al. 2006; Alsolmy et al. 2018). Another interesting application is fire retardancy using polymeric materials. In a polymer nanocomposite, organo-silicates can develop a ceramic superficial layer during the early stages of combustion, thereby protecting the underlying material by limiting heat transfer as well as hampering the diffusion of oxygen and the evacuation of combustible products (Fina et al. 2006). A tuneable refractive index has been achieved by modulating the concentration of phenyl groups (Lin et al. 2018). By optimizing the matrix structure, refractive indexes of hybrid silica are comparable to systems that employ zirconium as a refractive index modifier (Jeong and Moon 2005).

Phenyl-silica xerogels have also been applied to separations of several binary mixtures, including benzene-toluene, m-xylene-benzene, m-xylene-toluene, water–ethanol, and carbon tetrachloride-dichloromethane (Moriones et al. 2011). Due to the enhanced interaction between phenyl groups on the analyte and the stationary phase, aromatic substances had a stronger affinity for the hybrid xerogels than the other analytes.

Electronic supplementary material The online version of this article (https://doi.org/10.1007/s10450-019-00075-9) contains supplementary material, which is available to authorized users.

✉ J. C. Echeverria
jesus.echeverria@unavarra.es

✉ J. J. Garrido
j.garrido@unavarra.es

[1] Departamento de Ciencias, Edif. Los Acebos, Universidad Pública de Navarra, Campus Arrosadía, 31006 Pamplona, Spain

[2] Institute for Advanced Materials, Edif. Jerónimo de Ayanz, Universidad Pública de Navarra, Campus Arrosadía, 31006 Pamplona, Spain

[3] Instituto Nacional del Carbon, CSIC, Apartado 73, 33080 Oviedo, Spain

Hybrid xerogels have also been used for the separation of hexane isomers and they were able to differentiate between the adsorption of the mono and the di-branched isomers (Fernandes et al. 2019).

Hybrid xerogel films prepared at pH 10 from phenyltriethoxysilane (PhTEOS) and tetraethylsilane (TEOS) mixtures with 30, 40, and 50% PhTEOS in the mixture of their silicon precursors have been used as fiber-optic sensing elements (Echeverria et al. 2017). The films were affixed at the end of optical fibers by the dip-coating technique. The response of each sensing element in the presence of n-hexane decreased with temperature, which denotes an exothermic process and confirms the role of adsorption in the overall performance of the sensing elements. From calibration curves at different temperatures, the isosteric adsorption enthalpies were obtained. The enthalpy change indicated that the adsorbent-adsorbate interaction prevailed at lower relative pressure, whereas condensation of n-hexane on the meso and macropores was the main mechanism at higher relative pressure.

The overall performance of the hybrid material strongly depends on the nature and number of the organic functional groups incorporated into the network of the host structure, as well as the size and shape of the pores (Pardo et al. 2011). The most common way to introduce the phenyl group into the silica network is through the use of a phenyltrialkoxysilane precursor mixed with another tetraalkoxysilane precursor. Depending on the molar ratio of the phenyl precursor and the reaction conditions in the sol–gel process, the phenyl group can either act as a matrix modifier or it can direct the formation of lamella (Shimojima et al. 1998) and smaller species such as cage structures or ladder-like polymers (Loy 2007). The phenyl group has steric effects that retard condensation reactions and induces the formation of cycles such as polyhedral oligosilsesquioxanes (Loy et al. 2000; Loy 2007). The organic groups in hydrolysed species act as blocking agents to shield one side of the monomer from reactions that would promote cyclation. However, as silanols are converted into siloxane bonds, the polysilsesquioxanes may become sufficiently hydrophobic to induce phase separation as a precipitate or resin rather than gelation (Loy 2007).

In this research we have investigated the effect of PhTEOS/tetraethoxysilane (TEOS) molar ratios as silicon precursors on the structure and porous texture of xerogels, with the aim of learning how to control the final properties of inorganic–organic materials derived from PhTEOS and TEOS.

2 Experimental section

2.1 Xerogels synthesis

PhTEOS and TEOS with purities of at least 98% were obtained from the Fluka Company (Switzerland). Absolute ethanol GR and aqueous ammonia GR for analysis were supplied by Merck (Darmstadt, Germany). Water was of MilliQ quality. All xerogels were synthesized at pH 10, 333 K, and a 1:6:6 precursor:ethanol:water molar ratio. The PhTEOS percentages in the siliceous mixture varied from 0 to 100%. The required amounts of precursors and ethanol were mixed using a magnetic stirrer in a 30-mL glass container. While stirring, the amount of water was added drop-wise, and the pH of the solution was adjusted to ten by adding 2-M $NH_{3(aq)}$ with an automated burette (Titrino 702 SM, Metrohm, Herisau, Switzerland). The sample containers were closed and stirred in an orbital shaker and then kept until gelation. The alcogels were covered with 5 mL of ethanol, allowed to age at room temperature for 7 days, and then dried at 295 ± 2 K under atmospheric pressure.

2.2 Sample characterization

The ^{29}Si cross-polarization magic angle spinning (CPMAS) solid-state NMR spectra were acquired on a Bruker AV-400 MHz spectrometer (Billerica, USA) operated at 79.5 MHz for ^{29}Si. The spectra were recorded at room temperature, with chemical shifts reported in ppm relative to tetramethylsilane (TMS). The sample-rotation frequency was 5 kHz for ^{29}Si. Classical notation was used for the ^{29}Si NMR studies: T for silicon with three bridging oxygen atoms (RTEOS) and Q for silicon with four bridging oxygen atoms (TEOS). T and Q notations are usually completed by an I index (T_i, i = 0, 1, 2 or 3; Qi, i = 0, 1, 2, 3 or 4), which represents the number of oxo bridges in Si–O–S– bonds. The ^{29}Si spectra were ^{1}H decoupled.

Fourier-transformed infrared (FTIR) spectra were obtained using a Nicolet Avatar 360 FTIR spectrometer (Madison, USA). For each sample, we recorded 32 scans in the 4000–400 cm^{-1} spectral range with a resolution of 4 cm^{-1}. The KBr pressed-disc technique was used at two sample concentrations: 2 and 0.6 mg dispersed in 198 and 199.4 mg of KBr, respectively. The first one provides detail in the 4000–2200 cm^{-1} region where hydroxyl and C-H bonds appear. The second one avoids signal saturation in the 2200–400 cm^{-1} range and makes it easier to analyse the bonds attributed to siloxanic structure. The discs were heated in a furnace at 423 K overnight to minimise the water adsorbed on KBr and the samples (Madejova and Komadel 2001).

X-ray diffraction (XRD) patterns were acquired at room temperature using a Rigaku D-max instrument (Rigaku, Tokio, Japan) with a copper rotating anode and a graphite monochromator, which was used to select the $CuK_{\alpha 1/2}$ wavelength. The device was used at 40 kV and 80 mA. The measurements were carried out in step-scan mode for $5° \leq 2\theta \leq 60°$, in steps of 0.03° with a counting rate of one step s^{-1}.

Journal : Large 10450 | Article No : 75 | Pages : 12 | MS Code : ADSO-D-18-00730 | Dispatch : 28-3-2019

Micrographs were obtained using a field-emission scanning electron microscope (FE-SEM) from Carl Zeiss Ultra Plus (Germany). This apparatus permits the observation of samples without metallic coatings. An InLens detector and a 2-kV working voltage were used. High-resolution transmission electron microscopy (HRTEM) images were obtained at 200 kV with a JEOL 2000 FXII microscope (0.28 nm point-to-point spatial resolution) equipped with an Oxford Instruments INCA 200 energy dispersive spectrometer.

Simultaneous thermogravimetry and differential scanning calorimetry (TGA-DSC) analyses of xerogels were performed using a thermogravimetric analyser SETARAM, Mod. Setsys Evolution 1600 (Caluire, France), under an air atmosphere. Samples were placed in a platinum crucible, and the heating rate was 10 K min^{-1}. A blank corresponding to a trial under the same conditions but without a sample was subtracted from each run.

The skeletal density was measured via helium pycnometry Accupyc 1330, Micromeritics (Norcross, Georgia, USA). Nitrogen adsorption at 77 K and CO_2 adsorption at 273 K were measured using an ASAP 2010 volumetric adsorption analyser from Micromeritics (Norcross, Georgia, USA). We obtained the adsorption–desorption isotherm of Ar at 87.3 K (ASAP 2020HD, Micromeritics, Norcross, Georgia, USA) for the xerogel synthesized from 50% PhTEOS to assess the contribution of quadrupolar moment of N_2 and CO_2 to the adsorption. Before adsorption analysis, the samples were outgassed for at least 15 h at 423 K at the degasification port of the adsorption apparatus with a residual vacuum of 7×10^{-1} Pa. Specific surface areas were calculated from the N_2 and Ar adsorption data (molecular cross section 0.162 nm^2 and 0.143 nm^2, respectively) by the Brunauer–Emmett–Teller (BET) method according to criteria described by Rouquerol et al. (Rouquerol et al. 1999), and by applying the Dubinin-Radushkevich (DR) method to CO_2 adsorption (molecular cross-section 0.187 nm^2). Total pore volume (V_t) was determined from the amount adsorbed at $p/p^o \sim 1$. Micropore volume was deduced by applying the DR method to N_2 ($V_{DR(N2)}$) and CO_2 ($V_{DR(CO2)}$) adsorption data. Mesopore volume (V_{meso}) values were obtained by subtracting the amount adsorbed at p/p^o 0.80 and 0.30. Macropore volume (V_{macro}) was obtained by difference between V_t and the amount adsorbed at p/p^o 0.80. Pore volumes were calculated using liquid-state densities for adsorbates of N_2 at 0.808 g cm^{-3} and CO_2 at 1.023 g cm^{-3} (Garrido et al. 1987; CazorlaAmoros et al. 1996).

3 Results and discussion

3.1 Gelation time

Gelation time (t_g) decreased with increasing PhTEOS molar ratio (Fig. S1). The sample prepared by using TEOS as the only silica precursor did not gel after 10 months due to the stability of the colloidal suspensions (Stöber et al. 1968; Celzard and Marêché 2002). On the other hand, hydrolysis and condensation of samples with 90 and 100% PhTEOS afforded precipitates (Loy et al. 2000; Dong et al. 2005). For mixtures PhTEOS/TEOS, t_g decreased according to a logarithmic relationship for molar ratios between 10 and 40%. For a PhTEOS concentration higher than 40%, t_g linearly decreased with time. Because gelation time as measured includes hydrolysis, condensation and colloid destabilization, the results suggest a change in the limiting step for molar ratios of PhTEOS higher than 40%. At pH 10 silanol groups dissociate and the negative charge stabilizes colloids. Therefore, the increase in the content of phenyl groups may favour the gelation of colloids by decreasing the surface charge density.

3.2 Structural characterization of xerogels

3.2.1 Nuclear magnetic resonance

Figure 1 shows the ^{29}Si NMR spectra for the xerogels obtained from 10, 20, 40, 50, 60 and 80% PhTEOS. It also includes the spectrum for one xerogel obtained from TEOS (0% PhTEOS) after adding NH_4F to induce the gelation of colloids. Ternary silicon species in which silicon atoms are bonded to phenyl groups are identified between −60 and −85 ppm, the maxima being located as follows: T^2, C_6H_5–Si≡$(O–Si)_2(OH)$ at −68.6 ppm and T^3, C_6H_5–Si≡$(O–Si)_3$ at −77.7 ppm. The presence of ternary signals proves that the bonds between silicon and carbon from the phenyl groups remains after hydrolysis and condensation reactions. Quaternary silicon species from TEOS appeared between −85 and −120 ppm, and the maxima were located as follows: Q^2, Si≡$(O–Si)_2(OH)_2$ at −92.0 ppm; Q^3, Si≡$(O–Si)_3(OH)$ at −101.3 ppm; and Q^4, Si≡$(O–Si)_4$ at −110.3 ppm (Vogt and Brown 1963; Brown et al. 1964; Innocenzi et al. 2003; Park et al. 2008; Koller and Ulke 2011; Rios et al. 2011). The smaller chemical shift of ternary silicon atoms in comparison to quaternary silicon proves that the phenyl group increases the partial negative charge of silicon atoms.

The relative intensity of the quaternary and ternary bands changed with the content of PhTEOS in the initial mixture of reagents (Figs. 1, 2). For percentages of the hybrid precursor equal or lower than 20%, quaternary signals were more intense than ternary signals, and Q^3 more intense than Q^4. For PhTEOS percentages equal or higher than 40%, ternary signals were more intense than quaternary, and T^3 predominated over T^2 signals. On the other hand, Q^4 became more intense than Q^3 as PhTEOS content increased. For 60 and 80% PhTEOS percentages, the Q^4 signal was stronger than Q^3.

Journal : Large 10450 | Article No : 75 | Pages : 12 | MS Code : ADSO-D-18-00730 | Dispatch : 28-3-2019

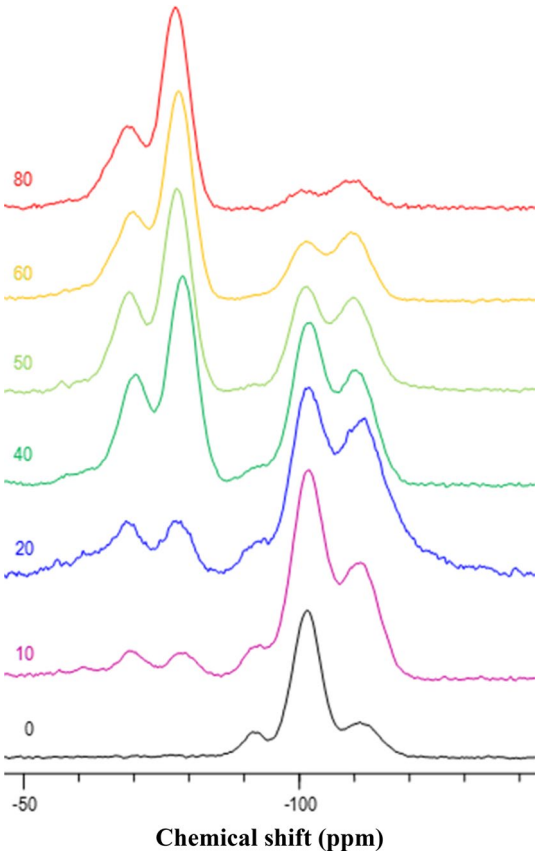

Fig. 1 Solid-state ^{29}Si NMR spectra of xerogeles synthesized from different molar percentage of PhTEOS (T^2, C_6H_5–Si≡(O–Si)$_2$(OH); T^3, C_6H_5–Si≡(O–Si)$_3$; Q^2, Si≡(O–Si)$_2$(OH)$_2$; Q^3, Si≡(O–Si)$_3$(OH); Q^4, Si≡(O–Si)$_4$)

According to Fig. 2a, the relative concentration of T^3, C_6H_5–Si≡(O–Si)$_3$, linearly increased with the PhTEOS content in the initial mixture of precursors, whereas the relative concentration of T^2, C_6H_5–Si≡(O–Si)$_2$(OH), species stabilized at around 20% for a PhTEOS percentage ≥ 50%. The relative concentration of less condensed species Q^2 and Q^3 signals decreased with an increasing PhTEOS content (Fig. 2b). In any case, T^2 and Q^3 were present even for xerogels formed from 80% PhTEOS, which provides evidence that silanol groups are present in the hybrid xerogels.

3.2.2 Infrared spectroscopy

FTIR provides complementary information to discern the bonding of silicon atom and the structure of xerogels. The FTIR spectra of the samples are included in the supplementary information (Fig. S2). The assignment of the bands shown in Table 1 was performed according to current literature (Bellamy 1975; Colthup et al. 1990; Ou and Seddon 1997; Fasce et al. 1999; Fidalgo and Ilharco 2001; Innocenzi 2003; Oubaha et al. 2005; Olejniczak 2005a, b; Al-Oweini and El-Rassy 2009; Li et al. 2009; Qin et al. 2011) and a multiple correlation analysis of the bands having higher intensity. The incorporation of phenyl groups into the structure of hybrid xerogels can be summarized by analysing the FTIR spectra at four wave ranges (Fig. S2): (a) 3800–2800 cm^{-1}, (b) 1800–1300 cm^{-1}, (c) 1300–900 cm^{-1}, and (b) 900–400 cm^{-1}. FTIR spectroscopy confirms the stability of the bond between silicon and a carbon atom from the phenyl group. The presence of the aromatic group resulted in several bands in the 3140–3010 cm^{-1} range, corresponding to stretching vibration of C–H bonds in the phenyl group (Bellamy 1975; Ou and Seddon 1997; Oubaha

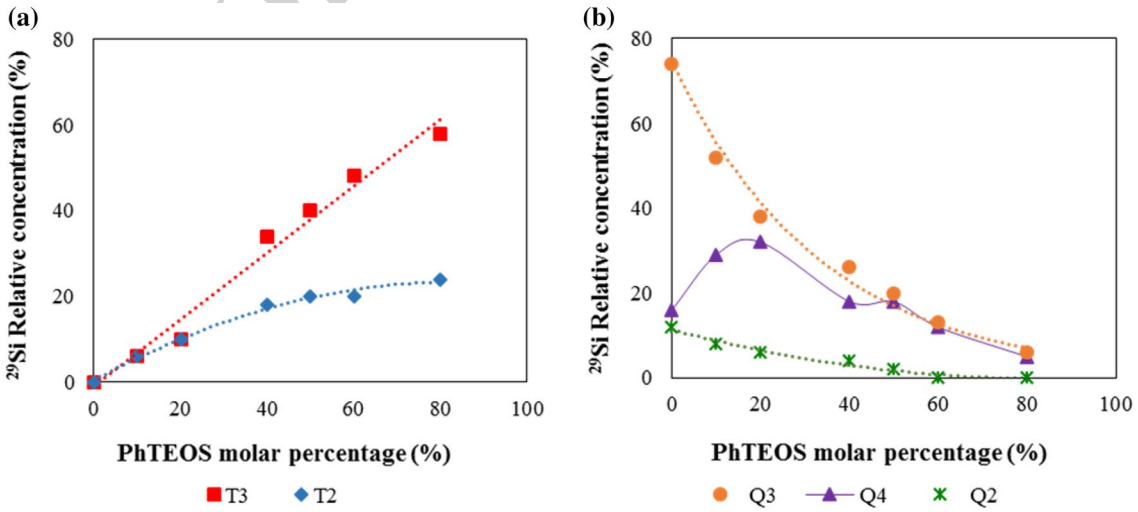

Fig. 2 Relative concentrations of ^{29}Si species in hybrid xerogels as a function of PhTEOS molar percentage: **a** ternary silicon species and **b** quaternary silicon species [T^2, C_6H_5–Si≡(O–Si)$_2$(OH); T^3, C_6H_5–Si≡(O–Si)$_3$; Q^2, Si≡(O–Si)$_2$(OH)$_2$); Q^3, Si≡(O–Si)$_3$(OH); Q^4, Si≡(O–Si)$_4$]

Journal : Large 10450 | Article No : 75 | Pages : 12 | MS Code : ADSO-D-18-00730 | Dispatch : 28-3-2019

Table 1 Characteristic vibration wavenumbers (cm^{-1}) in FTIR spectra of phenyl functionalized hybrid silica xerogels

Wavenumber (cm^{-1})	Type of vibration	Structural unit
3641	ν OH, H	SiO–H
3427	ν (SiO–H, H)	SiO–H–H
3140	ν (C–H)	C=C–H
3090	ν (C–H)	C=C–H
3078	ν (C–H)	C=C–H
3056	ν (C–H)	C=C–H
3032	ν (C–H)	C=C–H
3018	ν (C–H)	C=C–H
3010	ν (C–H)	C=C–H
2987	ν_{as} (C–H)	$–CH_3$
2931	ν_{as} (C–H)	$–CH_2–R$
2906	ν_s (C–H)	CH_3 terminal
1595	ν (C=C)	$–C_6H_5$
1431	ν (C=C)	$–C_6H_5$
1234	ν_{as} Si–O–Si (mode LO)	≡Si–O–Si≡
1134	ν Si–O–Si	≡Si–O–Si≡ (T_8)
1097	ν_{as} Si–O–Si (mode TO)	≡Si–O–Si≡
999	ν_s C=C	$–C_6H_5$
958	ν_{as} (Si–OH)	≡Si–OH
800	ν_s Si–O	≡Si–O–Si Si≡
739	$_{T\delta,y}$ C–H	$–C_6H_5$
698	Φ C–H	$–C_6H_5$
563	ν Si–O	SiO_2
474	Φ C–H	$–C_6H_5$
463	δ Si–O–Si	–O–Si–O–

ν stretching vibration; ν_s symmetric stretching vibration; ν_{as} antisymmetric stretching vibration; $_{\delta}$, deformation vibration; T_{δ} in-phase out-of-plane wagging; M, out-of-plane ring deformation vibration; $T_{8,}$ cubic octamer.

et al. 2005; Li et al. 2009). Specifically, a doublet with the largest intensity at ~3074 and 3051 cm^{-1}; another doublet of low intensity at ~3140 and 3090 cm^{-1}, and a triplet of medium intensity at ~3039, 3016 and 3007 cm^{-1}; which are related to several C–H stretching modes. The bands in the 1800–1300 cm^{-1} range are attributed to the stretching vibration of a phenyl framework (Lin et al. 2018). Several vibration modes of phenyl groups bonded to silicon (Si–C) appeared at ~999, 739, 698 and 474 cm^{-1} (Bellamy 1975; Colthup et al. 1990; Ou and Seddon 1997; Fidalgo and Ilharco 2001; Olejniczak et al. 2005a, b; Fina et al. 2006; Al-Oweini and El-Rassy 2009; Li et al. 2009).

The SiO_2 network changed when increasing PhTEOS content (Innocenzi 2003; Fidalgo and Ilharco 2004) (Fig S3). This figure includes the variation of absorbance as a function of wavenumber, as well as the first and second derivative of the absorbance. As PhTEOS content went up, the 1097 cm^{-1} band and the shoulder at 1234 cm^{-1}, which are associated with the siloxane bond in amorphous gels, decreased in intensity, and a narrow band appeared at 1134 cm^{-1}, whose absorbance increased with the concentration of the hybrid precursor. Although the band at 1134 cm^{-1} has been taken as evidence for the presence of strainless cage structures of the T_8–T_{14} type (Vogt and Brown 1963; Brown et al. 1964; Fasce et al. 1999; Dong et al. 2005; Qin et al. 2011) and highly symmetrical structure with $(Si–O)_4$ ring subunits (Park et al. 2008), this band is also found in the spectra of liquid PhTEOS used as precursor.

Another relevant effect of increasing the PhTEOS molar ratio is the decrease in intensity of the band with a maximum at around 3414 cm^{-1}, which is attributed to different contributions of geminal, vicinal and H-bonding silanol groups (Colthup et al. 1990; Fidalgo and Ilharco 2001; Innocenzi 2003; Innocenzi et al. 2003; Olejniczak et al. 2005a, b; Oubaha et al. 2005). In any case, isolated silanol groups (Colthup et al. 1990; Fidalgo and Ilharco 2001; Innocenzi et al. 2003; Oubaha et al. 2005) remained in the hybrid xerogels even for PhTEOS molar ratios as high as 80%, which is confirmed by the presence of the band at 3641 cm^{-1}. The presence of these bands backs up the results described in the Sect. 3.2.1 devoted to ^{29}Si NMR.

3.2.3 X-ray diffraction spectroscopy

X-ray diffraction patterns for samples synthesized from 10, 20, 40, 50, 60, and 80% PhTEOS molar percentages are shown in Fig. 3a. All patterns show one broad peak, characteristic of amorphous silica materials (Kamiya et al. 1998; Garcia-Cerda et al. 2002), with a maximum that shifted from 2θ ~ 22.2º for 10% PhTEOS to 2θ ~ 19.3° for 80% PhTEOS. For PhTEOS molar ratios equal or higher than 40%, a distinct peak developed, whose maximum varied from 2θ ~ 6.3º for 40% PhTEOS to 2θ ~ 7.2º for 80% PhTEOS. Figure 3b shows the variation of the d-spacing deduced from the two bands as a function of the molar percentage of the hybrid precursor.

The broad peak between 19.3° and 22.2° is related to the spacing between silicon atoms connected by means of an oxygen bridge (Lana and Seddon 1998). This distance increased from 0.40 nm for the silica xerogel synthesized from 10% PhTEOS to 0.46 nm for 80% PhTEOS. The shift of this band is attributed to steric and inductive effects of the intercalated phenyl groups in the matrix of siloxane bonding, as demonstrated by the T^2 and T^3 signals in the ^{29}Si NMR spectra.

On the other hand, the peak that appeared at 2θ < 10° became sharper and shifted to a wider angle with increasing PhTEOS concentration. Bragg d-spacing decreased from 1.41 nm for 40% PhTEOS to 1.23 nm for 80% PhTEOS (Fig. 3b). The origin of this peak is still controversial. It has been assigned to the presence of fourfold

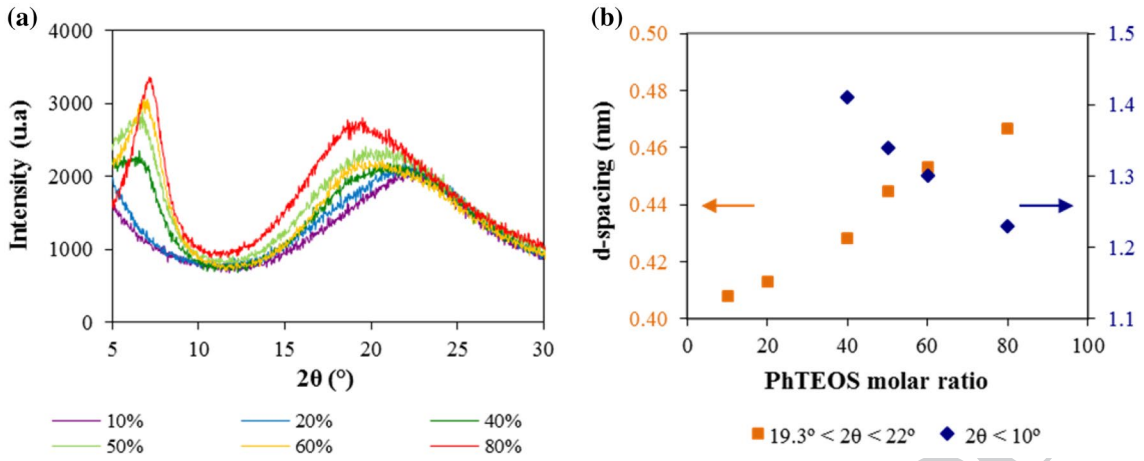

Fig. 3 **a** X-ray diffraction patterns of selected hybrid xerogeles, and **b** d-spacing deduced from the two bands as a function of PhTEOS molar percentages

siloxane rings (Yoshino et al. 1990; Kamiya et al. 1998; Fidalgo and Ilharco 2001), but it may originate in a discrete structural unit in the matrix based on an octameric silicon arrangement (Lana and Seddon 1998; Orel et al. 2005). While tetraalkoxysilanes like TEOS undergo intermolecular branching and gelation, enhancing steric hindrance—due to a bulky organic group such as phenyl—strongly favors an intramolecular reaction and cyclics formation at the expense of intermolecular condensation (Zhang et al. 2006, 2008; Alauzun et al. 2008; Choi et al. 2011). Gelation would confirm that ordered domains are embedded in amorphous oligomers (Loy 2007).

Another hypothesis is that the structure consists of a siloxane network and organic layers containing ordered arrangements. The self-assembly process from co-condensation of PhTEOS and TEOS can be summarized in three imbricated steps. Hydrolysis of the hybrid precursor results in amphiphilic species that include hydrophilic silanols and hydrophobic phenyl groups. The amphiphilic species then assemble and organize themselves into a solid cross-linked mesostructure through condensation. The presence of strong van der Waals binding organic groups drives the self-assembly process (Shimojima et al. 1998, 2005; Chemtob et al. 2014). The decrease in d-spacing from 1.41 nm for 40% PhTEOS to 1.23 nm for 80% PhTEOS could be due to a reduction in the thickness of the amorphous silica layer when the molar ratio of TEOS goes down and the PhTEOS percentage goes up. The basic aggregates of amphiphilic molecules, such as the hydrolysis products $C_6H_5Si(OH)_3$, is related to the ratio of the volume of the molecule to the product of the surface area and the maximum extension of the non-polar group (Piazza 2010). For bulky groups, like the phenyl group, the formation of lamellar structures is favoured.

3.2.4 TEM and FE-SEM micrographs

The nanostructures of these hybrid materials were also studied using TEM (Fig. 4). The micrographs show the evolution in the nanostructures of the xerogels. The sample prepared from 20% PhTEOS and 80% TEOS was made up of aggregates of nanoparticles having around 20 nm in size, with pores of similar dimensions. The size of the aggregates increased with the molar percentage of the hybrid precursor, and the nanostructure changed from aggregates of nanoparticles to lamellae, which are patent for 60% and 80% samples. Therefore, the TEM-micrographs confirm the formation of ordered domains shown in the X-ray diffractograms.

Figure 5 shows FE-SEM images of xerogels at different molar ratios of PhTEOS: (a) 20%, (b) 40%, (c) 60%, and (d) 80%. When the PhTEOS content as silicon precursors increased, the morphology of xerogels changed from aggregates of spherical particles for 20% PhTEOS to large lumps of fused spheres where single particles could not be distinguished for the xerogels obtained with 80% PhTEOS. Along with the tendency to coalesce, average pore size and pore size distribution became wider with an increasing molar ratio of the hybrid precursor. Mean particle size and pore size were estimated by averaging 25 single measurements ("NIS Elements. Advanced solutions for your imaging world." 2010). Mean particle size was 42 ± 4 nm for 20% PhTEOS, 36 ± 11 nm for 40%, 34 ± 3 nm for 60% and > 1000 nm for 80%. Average pore sizes were 60 ± 10 for 20% PhTEOS, 69 ± 23 nm for 40% nm, 56 ± 7 nm for 60%, and > 500 nm for 80%.

Journal : Large 10450 | Article No : 75 | Pages : 12 | MS Code : ADSO-D-18-00730 | Dispatch : 28-3-2019

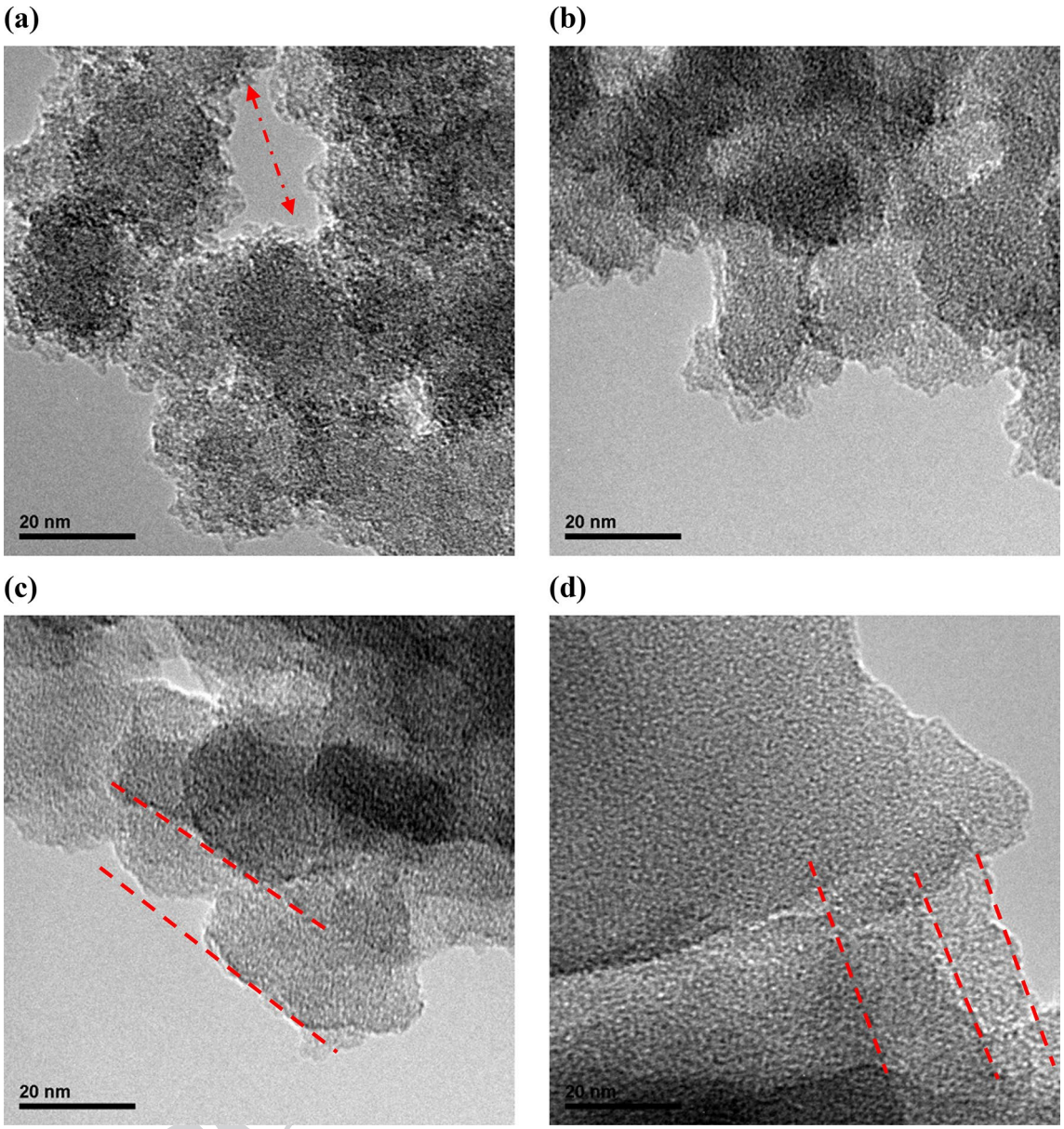

Fig. 4 TEM micrographs of hybrid xerogeles: **a** 20% PhTEOS, **b** 40% PhTEOS, **c** 60% PhTEOS, and **d** 80% PhTEOS

3.2.5 Thermogravimetric analysis and differential scanning calorimetry

Figure 6a shows TGA curves of xerogels synthesised from PhTEOS molar ratios ranging from 10 to 80%. Thermograms present three temperature steps which correspond to different processes. The first step goes up to 573 K, and DSC analysis confirms that it is an endothermic process. Mass loss decreased with PhTEOS molar ratio from 7.7% for 10% PhTEOS to 5.1% for 80% (Fig. 6b). This weight loss can be attributed to the removal of physisorbed molecules, in particular, water and ethanol entrapped in the pores. Superficial silanol groups have greater affinity for water and polar solvents than phenyl groups, and consequently the slope of the curves and the magnitude of the changes in mass in this step suggest that surface polarity decreases with increasing PhTEOS molar ratio. The second step ranges from 573 to 773 K and mass loss varied between 3 and 4%, without significant differences in samples. It can be assigned to the loss of residual ethoxy groups and water produced by condensation of silanol groups on the surface. The third step takes place at a temperature higher than 773 K. The mass loss increased with PhTEOS content from 8.2% for 10% PhTEOS to 40.8% for 80% PhTEOS. This process is exothermic and corresponds to the oxidation of phenyl groups into CO_2 and H_2O.

Journal : Large 10450 | Article No : 75 | Pages : 12 | MS Code : ADSO-D-18-00730 | Dispatch : 28-3-2019

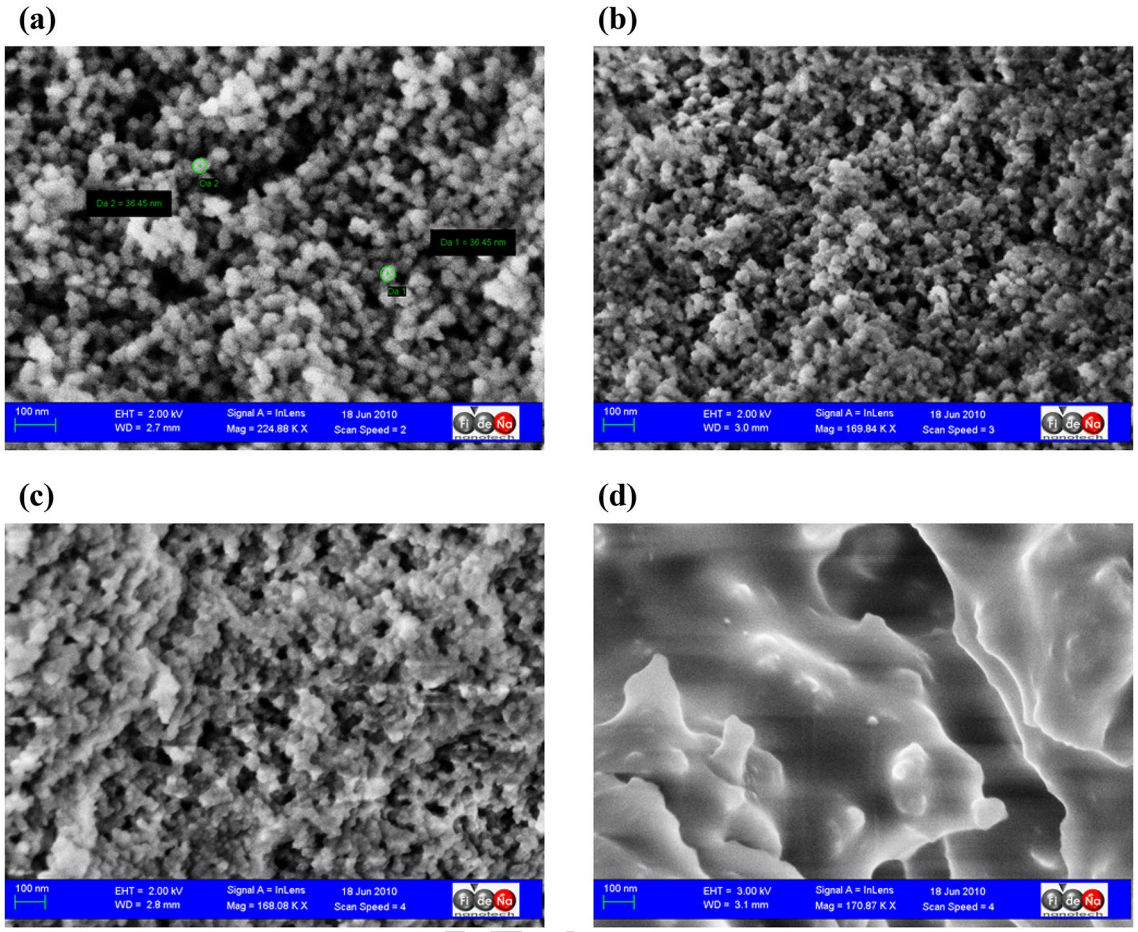

Fig. 5 FE-SEM images of hybrid xerogels synthesized with different percentages of PhTEOS: **a** 20%, **b** 40%, **c** 60% and **d** 80%

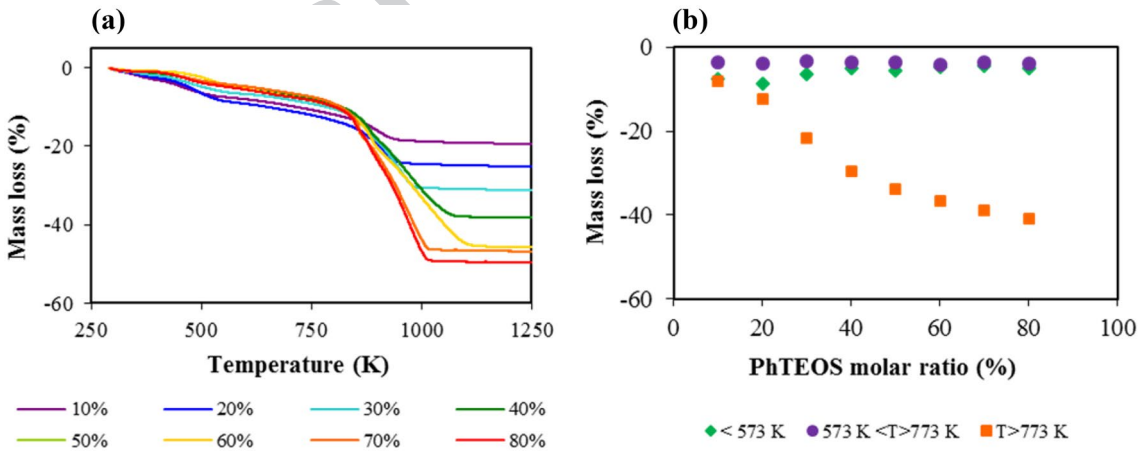

Fig. 6 **a** TGA and **b** The mass loss (%) as a function PhTEOS molar percentage. Heating rate was 10 K min^{-1} under air atmosphere

3.3 The porous texture of xerogels

The helium density of hybrid xerogels decreased with the amount of PhTEOS and ranged from 1.924 g cm^{-3} for the xerogel synthesized from 10% PhTEOS to 1.393 g cm^{-3} for the xerogel synthesised from 80% PhTEOS (Fig. S4). The plot of d_{He} as a function of the molar percentage of the hybrid precursors shows that the experimental data can be fitted to

Journal : Large 10450 | Article No : 75 | Pages : 12 | MS Code : ADSO-D-18-00730 | Dispatch : 28-3-2019

two linear ranges: between a 10 and 40% PhTEOS molar ratio the slope of the linear equation is -1.3×10^{-2} g cm^{-3} %$^{-1}$; and between 40 and 80% it is -3.8×10^{-3} g cm^{-3} %$^{-1}$. The decrease in d_{He} is related to the incorporation of phenyl groups in the xerogel. The fact that the slope of the variation of d_{He} was lower in the range 40–80% than between 10 and 40% indicates the contribution of another effect, which could be the apparition of lamellar domains in the xerogels that has been discussed in Sect. 3.2.4 devoted to TEM analysis.

3.3.1 Adsorption–desorption isotherms

Figure 7 shows the adsorption–desorption isotherms of the hybrid xerogels synthesized in the range 10–80% PhTEOS molar ratios: (a) N_2 at 77 K and (b) CO_2 at 273 K. The insert shows the relative pressure in a logarithmic scale to detail the adsorption of N_2 at p/p° below 0.1. The amount of N_2 adsorbed decreased with an increase in content of the hybrid precursor, and the isotherm knee became sharper. The xerogel synthesized from 80% PhTEOS scarcely adsorbed N_2 at 77 K. Differences in the adsorbed amount were more marked for molar ratios higher than 50% and relative pressure below 0.1. Except for 80% PhTEOS, all xerogels presented N_2 isotherms belonging to Type IV of the IUPAC classification (Thommes et al. 2015). Type IV isotherms are given by meso- and macroporous adsorbents. The adsorption behaviour in meso and macropores is determined by the adsorbent-adsorptive interactions and by the interactions between the molecules in the condensed state. In the case of a Type IVa isotherm, capillary condensation is accompanied by hysteresis. This occurs when the pore width exceeds a certain critical width, which is dependent on the adsorption system and temperature (Thommes et al. 2015). The fact that the samples adsorbed much more N_2 at relative pressure p/p° > 0.1 than at p/p° < 0.1 confirms that xerogels are mainly meso- and macroporous materials.

For PhTEOS molar ratios equal or lower than 50%, hysteresis loops are type H1, The Type H1 loop is found in materials which exhibit a narrow range of uniform pores. Usually, network effects are minimal and the steep, narrow loop is a clear sign of delayed condensation on the adsorption branch (Thommes et al. 2015). Xerogels synthesized by using 60 and 70% PhTEOS molar ratios presented hysteresis loops Type H2 that have the desorption branch steeper than the adsorption one. The Type H2(b) loop is also associated with pore blocking, but the size distribution of neck widths is now much larger. Examples of this type of hysteresis loops have been observed with mesocellular silica foams and certain mesoporous ordered silicas after hydrothermal treatment.

The adsorption of CO_2 also decreased with the molar percentage of PhTEOS, but without discontinuity between 50 and 60% as in N_2 isotherms. CO_2 isotherms cover relative pressures up to 0.03, because the CO_2 saturation pressure at 273 K is 34.4 bar.

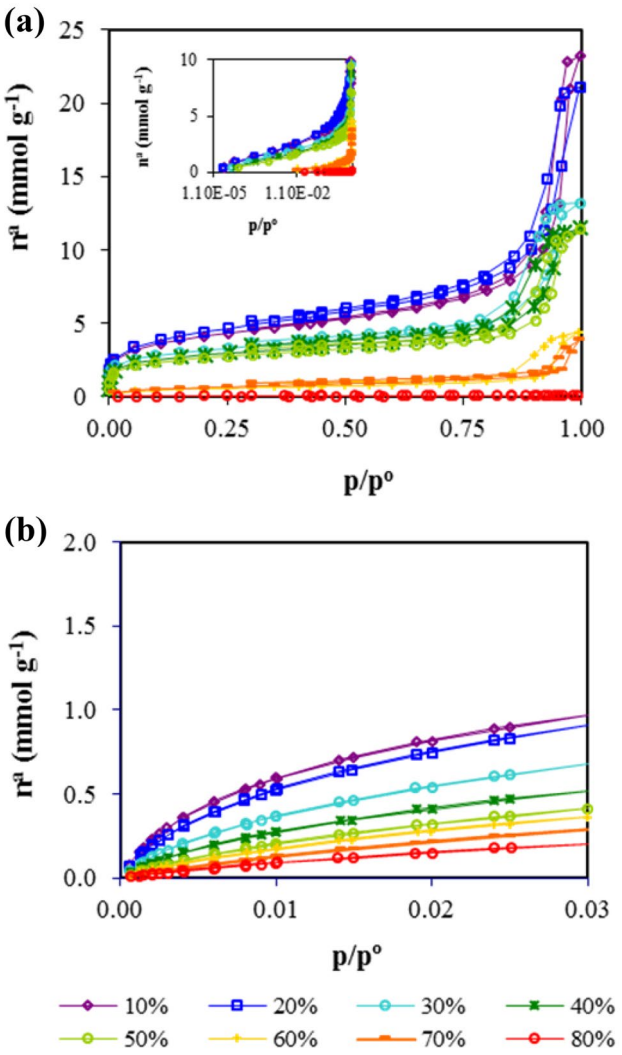

Fig. 7 Adsorption isotherms **a** N_2 at 77 K **b** CO_2 at 273 K. The insert plots the relative pressure in logarithmic scale to detail the adsorption at relative pressure below 0.1

The adsorption isotherms and the thermal analysis reveal that an increase in the molar percentage of the hybrid precursor brings about a change in the surface chemistry, so xerogels became more hydrophobic, and there is a reduction in the amount of N_2 and CO_2 adsorbed.

3.3.2 Specific surface area

The textural parameters deduced from the N_2 and CO_2 adsorption data are included in Table 2. Correlation analysis of the precursor molar percentages and the textural parameters revealed that increasing PhTEOS in the mixture of silicon precursors produced hybrid xerogels with lower specific surface area, pore volume, and characteristic energy

than a xerogel synthesized from TEOS (Table S1). Specific surface areas deduced by applying the BET method to N_2 adsorption data ($a_{s(BET-N2)}$) ranged from 340 $m^2\ g^{-1}$ for 20% PhTEOS to 4 $m^2\ g^{-1}$ for 80%. The experimental values confirm that the specific area reduction was larger between 50 and 60% PhTEOS. The decrease in the amount of adsorbed N_2 could be attributed to the weaker cross-linking and the associated gel flexibility that collapses local domains. At larger percentages of PhTEOS, it could also be attributed to the formation of lamellar domains that has been confirmed by XRD and TEM.

In order to assess the contribution of the quadrupolar moment of N_2 and CO_2 to the adsorption, we obtained the adsorption–desorption isotherm of Ar at 87.3 K for the xerogel synthesized from 50% PhTEOS (Fig. S5). Adsorption–desorption isotherms of N_2 and Ar are Type IV—the knee, the plateau and the amount adsorbed are similar for Ar and N_2. The specific surface area was 219 $m^2\ g^{-1}$ for Ar and 209 $m^2\ g^{-1}$ for the $a_{BET\ (N2)}$. This similarity indicates that physisorption is the main retention mechanism, and that the variation in the surface chemistry with the incorporation of phenyl groups does not inhibits the retention of N_2.

3.3.3 Pore volumes

Figure 8 shows the variation of the total pore volume (V_t), as well as the volume of macro (V_{macro}), meso (V_{meso}) and micropores (V_{micro}) as a function of the PhTEOS molar percentage in the initial mixture of precursors. The total volume of pores was obtained by converting the amount adsorbed at the isotherm plateau into a volume of liquid, assuming that the density of the adsorbate is equal to the bulk liquid density at saturation (Lowell et al. 2006). The total pore volume decreased from 0.805 $cm^3\ g^{-1}$ for 10% PhTEOS to 0.005 $cm^3\ g^{-1}$ for 80% PhTEOS. Comparison of volume of macro-, meso- and micropores reveals that macropores are the main contributors to porosity because they account for more than 60% of the total pore volume (Fig. 8). The volume of mesoporos steadily decreased along with the PhTEOS percentage and comprised between 10 and 15% of total

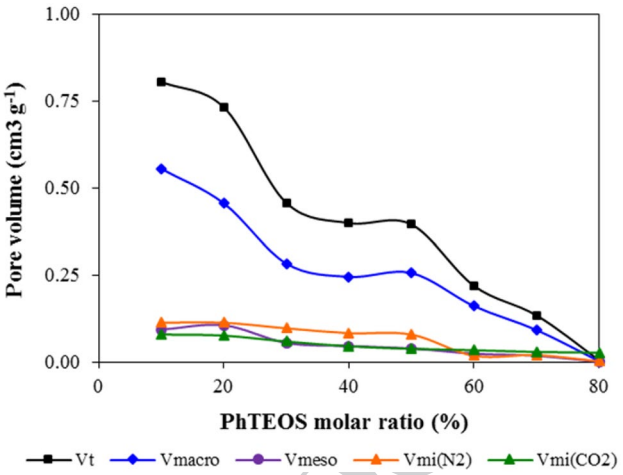

Fig. 8 Pore volume of xerogels as a function of molar percentage of PhTEOS

porosity. Both $V_{micro(N2)}$ and $V_{micro(CO2)}$ decreased with the incorporation of phenyl groups in the xerogel. $V_{micro(N2)}$ was larger than $V_{micro(CO2)}$ for PhTEOS percentages between 10 and 50%, but for larger percentages of the hybrid precursor the trend reversed, which reflects the change in the properties of the surface of xerogels. These results agree with those described in the sections devoted to FE-SEM images (Fig. 5), which showed that interparticle volume constitutes the main contribution to total pore volume and macropore volume.

3.3.4 Characteristic energy

For each adsorbate, the characteristic energy decreased with PhTEOS content, the effect being larger for $Ec_{(N2)}$ than for $Ec_{(CO2)}$ (Table 2). FTIR spectra demonstrated the incorporation of phenyl groups into the xerogel and the modification of siloxane bonds. Phenyl groups on the surface decreased the surface polarity, which would result in lower characteristic energy. In short, PhTEOS gave rise to xerogels that were less polar than those obtained from TEOS and, consequently,

Table 2 Textural parameters of phenyl-functionalized hybrid xerogels prepared at pH 10 from mixtures of PhTEOS and TEOS

PhTEOS (%)	Specific area ($m^2\ g^{-1}$)		Pore volume ($cm^3\ g^{-1}$)				E_c (kJ mol^{-1})	
	$a_{BET\ (N2)}$	$a_{DR\ (CO2)}$	Total	$V_{DR(N2)}$	$V_{DR(CO2)}$	Mesopores	N_2	CO_2
10	321	145	0.805	0.113	0.079	0.154	16.7	20.8
20	340	144	0.795	0.113	0.075	0.178	16.3	20.3
30	245	117	0.458	0.097	0.059	0.129	16.0	19.4
40	227	94	0.398	0.083	0.046	0.104	15.8	19.1
50	209	85	0.395	0.080	0.039	0.081	14.3	18.2
60	43	80	0.153	0.018	0.036	0.031	10.3	17.7
70	51	78	0.134	0.020	0.034	0.026	10.0	16.6
80	4	61	0.005	0.001	0.026	0.001	8.5	16.0

Journal : Large 10450 | Article No : 75 | Pages : 12 | MS Code : ADSO-D-18-00730 | Dispatch : 28-3-2019

showed lower chemical interaction between adsorbent and adsorbate, and lower the characteristic energy.

The correlation coefficient for E_c from N_2 and CO_2 was 0.95 (Table S1). When correlation analysis was extended to specific surface area and pore volume, characteristic energy obtained from CO_2 adsorption presented correlation coefficients higher that 0.91 for all textural parameters. On the other hand, E_c from N_2 adsorption only correlated with $a_{s(BET)}$. Therefore, the characteristic energy determined from CO_2 adsorption appears to be a better indicator of textural parameters than $E_{c(N2)}$.

4 Conclusions

AQ2 We have investigated the structure and porous texture of phenylsilane hybrid xerogels prepared from mixtures of PhTEOS and TEOS. The gelation time decreased with an increasing PhTEOS molar ratio at pH 10. Increasing the concentration of phenyl groups yielded colloids with a lower density in silanol groups which, in turn, reduced the surface charge density of colloids and favoured gelation. The morphology of xerogels changed from aggregates of spherical particles for 20% PhTEOS to lamellae for samples obtained with PhTEOS percentages equal or larger that 60%. An incorporation of phenyl groups into the xerogel matrix caused an increase in the spacing bond between silicon atom and promoted an intramolecular reaction and the formation of lamellar domains. FTIR spectra demonstrate that the incorporation of phenyl groups reduces the amount of hydroxyl groups. Phenyl-silica xerogels were thermostable up to 773 K. Increasing the PhTEOS molar ratio in the mixture of silicon precursors produced hybrid xerogels with lower specific surface area, pore volume and characteristic energy. The similarity between the isotherms of N_2 at 77 K and Ar at 87.3 K indicates that the main retention mechanism is physisorption, and that the variation in the surface chemistry with the incorporation of phenyl groups does not inhibit the retention of N_2.

Acknowledgements This work was backed by the "Ministerio de Ciencia y Tecnología" (Grant No. CTQ2009-07993) and by the "Ministerio de Economía, Industria y Competitividad" (Grant No. MAT2016-78155-C2-2-R). Paula Moriones is grateful to the "Departamento de Industria y Tecnología, Comercio y Trabajo" of the Navarre Government for the fellowships granted (Ref. Number 175/01/08 and 269/01/08, respectively). The authors thank the "Servicios Científico-Técnicos de Investigación" at the University of Cantabria (Spain) for TGA-DSC analysis.

References

Alauzun, J., Mehdi, A., Mouawia, R., Reyé, C., Corriu, R.: Synthesis of new lamellar materials by self-assembly and coordination chemistry in the solids. J. Sol-Gel. Sci. Technol. **46**, 383–392 (2008)

Al-Oweini, R., El-Rassy, H.: Synthesis and characterization by FTIR spectroscopy of silica aerogels prepared using several $Si(OR)_4$ and R ''$Si(OR')_3$ precursors. J. Mol. Struct. **919**, 140–145 (2009)

Alsolmy, E., Abdelwahab, W.M., Patonay, G.: A comparative study of fluorescein Isothiocyanate-encapsulated silica nanoparticles prepared in seven different routes for developing fingerprints on non-porous surfaces. J. Fluoresc **28**, 1049–1058 (2018)

Bellamy, L.J.: The Infra-Red Spectra of Complex Molecules. Springer, New York (1975)

Brown, J.F., Vogt, L.H., Prescott, P.I.: Preparation and characterization of lower equilibrated phenylsilsesquioxanes. J. Am. Chem. Soc. **86**, 1120–1125 (1964)

CazorlaAmoros, D., AlcanizMonge, J., LinaresSolano, A.: Characterization of activated carbon fibers by CO_2 adsorption. Langmuir **12**, 2820–2824 (1996)

Celzard, A., Marêché, J.F.: Applications of the sol-gel process using well-tested recipes. J. Chem. Educ. **79**, 854–859 (2002)

Chemtob, A., Ni, L.L., Croutxe-Barghorn, C., Boury, B.: Ordered hybrids from template-free organosilane self-assembly. Chem. Eur. J. **20**, 1790–1806 (2014)

Choi, S.-S., Lee, A., Lee, H., Baek, K.-Y., Choi, D., Hwang, S.: Synthesis and characterization of ladder-like structured polysilsesquioxane with carbazole group. Macromol. Res. **19**, 261–265 (2011)

Colthup, N.B., Daly, C.M., Wiberley, S.E.: Introduction to Infrared and Raman Spectroscopy. Academic Press, New York (1990)

Dong, H.J., Brook, M.A., Brennan, J.D.: A new route to monolithic methylsilsesquioxanes: gelation behavior of methyltrimethoxysilane and morphology of resulting methylsilsesquioxanes under one-step and two-step processing. Chem. Mater. **17**, 2807–2816 (2005)

Echeverria, J.C., Calleja, I., Moriones, P., Garrido, J.J.: Fiber optic sensors based on hybrid phenyl-silica xerogel films to detect n-hexane: determination of the isosteric enthalpy of adsorption. Beilstein J. Nanotech. **8**, 475–484 (2017)

Fasce, D.P., Williams, R.J.J., Mechin, F., Pascault, J.P., Llauro, M.F., Petiaud, R.: Synthesis and characterization of polyhedral silsesquioxanes bearing bulky functionalized substituents. Macromolecules **32**, 4757–4763 (1999)

Fernandes, J., Fernandes, A.C., Echeverria, J.C., Moriones, P., Garrido, J.J., Pires, J.: Adsorption of gases and vapours in silica based xerogels. Colloids Surf. Physicochem. Eng. Asp. **561**, 128–135 (2019)

Fidalgo, A., Ilharco, L.M.: The defect structure of sol-gel-derived silica/polytetrahydrofuran hybrid films by FTIR. J. Non-Cryst. Solids **283**, 144–154 (2001)

Fidalgo, A., Ilharco, L.M.: Correlation between physical properties and structure of silica xerogels. J. Non-Cryst. Solids **347**, 128–137 (2004)

Fina, A., Tabuani, D., Carniato, F., Frache, A., Boccaleri, E., Camino, G.: Polyhedral oligomeric silsesquioxanes (POSS) thermal degradation. Thermochim. Acta **440**, 36–42 (2006)

Garcia-Cerda, L.A., Mendoza-Gonzalez, O., Perez-Robles, J.F., Gonzalez-Hernandez, J.: Structural characterization and properties of colloidal silica coatings on copper substrates. Mater. Lett. **56**, 450–453 (2002)

Garrido, J., Linares-Solano, A., Martin-Martinez, J.M., Molina-Sabio, M., Rodriguez-Reinoso, F., Torregrosa, R.: Use of N_2 vs CO_2 in the characterization of activated carbons. Langmuir **3**, 76–81 (1987)

Innocenzi, P.: Infrared spectroscopy of sol-gel derived silica-based films: a spectra-microstructure overview. J. Non-Cryst. Solids **316**, 309–319 (2003)

Innocenzi, P., Falcaro, P., Grosso, D., Babonneau, F.: Order-disorder transitions and evolution of silica structure in self-assembled

mesostructured silica films studied through FTIR spectroscopy. J. Phys. Chem. B **107**, 4711–4717 (2003)
Jeong, S., Moon, J.: Fabrication of inorganic-organic hybrid films for optical waveguide. J. Non-Cryst. Solids **351**, 3530–3535 (2005)
Kamiya, K., Dohkai, T., Wada, M., Hashimoto, T., Matsuoka, J., Nasu, H.: X-ray diffraction of silica gels made by sol-gel method under different conditions. J. Non-Cryst. Solids **240**, 202–211 (1998)
Koller, H., Ulke, S.: Microheterogeneity in phenyl group modified inorganic/organic hybrid gels after aerosol drying or slow solvent evaporation. Solid State Nucl. Magn. Reson. **39**, 142–150 (2011)
Lana, S.L.B., Seddon, A.B.: X-ray diffraction studies of sol-gel derived ORMOSILs based on combinations of tetramethoxysilane and trimethoxysilane. J. Sol-Gel. Sci. Technol. **13**, 461–466 (1998)
Levy, D., Pardo, R., Zayat, M.: Photostability of a photochromic naphthopyran dye in different sol-gel prepared ormosil coatings. J. Sol-Gel. Sci. Technol. **40**, 365–370 (2006)
Li, Y.-S., Wang, Y., Ceesay, S.: Vibrational spectra of phenyltriethoxysilane, phenyltrimethoxysilane and their sol-gels. Spectrochim. Acta A **71**, 1819–1824 (2009)
Lin, W.S., Zheng, J.X., Zhuo, J.N., Chen, H.X., Zhang, X.X.: Characterization of sol-gel ORMOSIL antireflective coatings from phenyltriethoxysilane and tetraethoxysilane: microstructure control and application. Surf. Coat. Tech. **345**, 177–182 (2018)
Lowell, S., Shields, J.E., Thomas, M.A., Thommes, M.: Characterization of Porous Solids and Powders: Surface Area, Pore Size and Density. Springer, Dordrecht (2006)
Loy, D.A.: Sol-Gel processing of hybrid organic-inorganic materials based on polysisesquioxanes. In: Kickelbick, G. (ed.) Hybrid Materials, pp. 225–254. Wiley-VCH Verlag, Weinheim (2007)
Loy, D.A., Baugher, B.M., Baugher, C.R., Schneider, D.A., Rahimian, K.: Substituent effects on the sol-gel chemistry of organotrialkoxysilanes. Chem. Mater. **12**, 3624–3632 (2000)
Madejova, J., Komadel, P.: Baseline studies of the clay minerals society source clays: infrared methods. Clays Clay Miner. **49**, 410–432 (2001)
Moriones, P., Rios, X., Echeverria, J.C., Garrido, J.J., Pires, J., Pinto, M.: Hybrid organic-inorganic phenyl stationary phases for the gas separation of organic binary mixtures. Colloids Surf. Physicochem. Eng. Asp. **389**, 69–75 (2011)
NIS Elements: Advanced Solutions for Your Imaging World. Nikon Corporation, Amstelveen (2010)
Olejniczak, Z., Leczka, M., Cholewa-Kowalska, K., Wojtach, K., Rokita, M., Mozgawa, W.: ^{29}Si MAS NMR and FTIR study of inorganic-organic hybrid gels. J. Mol. Struct. **744–747**, 465–471 (2005a)
Olejniczak, Z., Cholewa-Kowalska, M.L.K., Wojtach, K., Rokita, M., Mozgawa W.: ^{29}Si MAS NMR and FTIR study of inorganic-organic hybrid gels. J. Mol. Struct. **744–747**, 465–471 (2005b)
Orel, B., Jese, R., Vilcnik, A., Stangar, U.L.: Hydrolysis and solvolysis of methyltriethoxysilane catalyzed with HCl or trifluoroacetic acid: IR spectroscopic and surface energy studies. J. Sol-Gel. Sci. Technol. **34**, 251–265 (2005)
Ou, D.L., Seddon, A.B.: Near- and mid-infrared spectroscopy of sol-gel derived ormosils: vinyl and phenyl silicates. J. Non-Cryst. Solids **210**, 187–203 (1997)
Oubaha, M., Etienne, P., Calas, S., Sempere, R., Nedelec, J.M., Moreau, Y.: Spectroscopic characterization of sol-gel organosiloxane materials synthesized from aliphatic and aromatic alcoxysilanes. J. Non-Cryst. Solids **351**, 2122–2128 (2005)
Pardo, R., Zayat, M., Levy, D.: Photostability of a photochromic naphthopyran dye in different sol-gel prepared ormosil coatings. J. Sol-Gel. Sci. Technol. **40**, 365–370 (2006)
Pardo, R., Zayat, M., Levy, D.: Photochromic organic-inorganic hybrid materials. Chem. Soc. Rev. **40**, 672–687 (2011)
Park, E.S., Ro, H.W., Nguyen, C.V., Jaffe, R.L., Yoon, D.Y.: Infrared spectroscopy study of microstructures of poly(silsesquioxane)s. Chem. Mater. **20**, 1548–1554 (2008)
Piazza, R.: Soft matter. The stuff dreams are made of. Springer, Dordrecht (2010)
Qin, Y., Ren, H., Zhu, F., Zhang, L., Shang, C., Wei, Z., Luo, M.: Preparation of POSS-based organic-inorganic hybrid mesoporous materials networks through Schiff base chemistry. Eur. Polym. J. **47**, 853–860 (2011)
Rios, X., Moriones, P., Echeverría, J.C., Luquin, A., Laguna, M., Garrido, J.J.: Characterisation of hybrid xerogels synthesised in acid media using methyltriethoxysilane (MTEOS) and tetraethoxysilane (TEOS) as precursors. Adsorption **17**, 583–593 (2011)
Rouquerol, F., Rouquerol, J., Sing, K.: Adsorption by Powders and Porous Solids. Academic Press, San Diego (1999)
Shimojima, A., Sugahara, Y., Kuroda, K.: Synthesis of oriented inorganic-organic nanocomposite films from alkyltrialkoxysilane-tetraalkoxysilane mixtures. J. Am. Chem. Soc. **120**, 4528–4529 (1998)
Shimojima, A., Liu, Z., Ohsuna, T., Terasaki, O., Kuroda, K.: Self-assembly of designed oligomeric siloxanes with alkyl chains into silica-based hybrid mesostructures. J. Am. Chem. Soc. **127**, 14108–14116 (2005)
Stöber, W., Fink, A., Bohn, E.: Controlled growth of monodisperse silica spheres in micron size range. J. Colloid Interface Sci. **26**, 62–69 (1968)
Thommes, M., Kaneko, K., Neimark, A.V., Olivier, J.P., Rodriguez-Reinoso, F., Rouquerol, J., Sing, K.S.W.: Physisorption of gases, with special reference to the evaluation of surface area and pore size distribution (IUPAC Technical Report). Pure Appl. Chem. **87**, 1051–1069 (2015)
Vogt, L.H., Brown, J.F.: Crystalline methylsilsesquioxanes. Inorg. Chem. **2**, 189–192 (1963)
Yoshino, H., Kamiya, K., Nasu, H.: IR study on the structural evolution of sol-gel derived SiO_2 gels in the early stage of conversion to glasses. J. Non-Cryst. Solids **126**, 68–78 (1990)
Zhang, X., Xie, P., Shen, Z., Jiang, J., Zhu, C., Li, H., Zhang, T., Han, C.C., Wan, L., Yan, S., Zhang, R.: Confined synthesis of a cis-isotactic ladder polysilsesquioxane by using a π-stacking and H-bonding superstructure. Angew. Chem. Int. Ed. **45**, 3112–3116 (2006)
Zhang, Z.X., Hao, J.K., Xie, P., Zhang, X.J., Han, C.C., Zhang, R.B.: A well-defined ladder polyphenylsilsesquioxane (Ph-LPSQ) synthesized via a new three-step approach: monomer self-organization-lyophilization-surface-confined polycondensation. Chem. Mater. **20**, 1322–1330 (2008)

Journal : **Large 10450** | Article No : **75** | Pages : **12** | MS Code : **ADSO-D-18-00730** | Dispatch : **28-3-2019**

Journal:	**10450**
Article:	**75**

Author Query Form

Please ensure you fill out your response to the queries raised below and return this form along with your corrections

Dear Author

During the process of typesetting your article, the following queries have arisen. Please check your typeset proof carefully against the queries listed below and mark the necessary changes either directly on the proof/online grid or in the 'Author's response' area provided below

Query	Details Required	Author's Response
AQ1	Author: Please check and confirm that the edit made in the title is correct.	
AQ2	Author: Reference Olejniczak et al. (2005) was repeated twice. Since we have changed to Olejniczak et al. (2005a) and Olejniczak et al. (2005b). Kindly check if action is appropriate.	